component $\mathbf{S}_{\|}$ tangential to $\mathcal{S}$ and a component $\mathbf{S}_{\perp}$ normal to $\mathcal{S}$, it follows with the aid of (11) and (14) that[10]

$$\mathbf{S}_{\|} = \rho_0 \frac{\partial \epsilon'}{\partial \mathbf{E}}, \quad \mathbf{E} \in \mathcal{S}. \tag{20}$$

We may regard the constrained material as a *constraint-manifold-Green-elastic* material: to each $\mathbf{E} \in \mathcal{S}$, the function ϵ' assigns a unique $\mathbf{S}_{\|}$ tangential to $\mathcal{S}$.

(c) If there is a second constraint of the type (2), the dimension of the manifold $\mathcal{S}$ is reduced to four, and two Lagrange multipliers will appear in the expression corresponding to (14); up to six (independent) constraints can be treated by this procedure, at which stage the material becomes rigidly constrained and $\mathbf{S}$ is completely indeterminate.

4 Cauchy-Elastic and Other Materials Subject to an Internal Constraint

For Cauchy-elastic materials, a constitutive function $\bar{\mathbf{S}}$ exists, but there may be no strain energy function. For such materials, the construction in Section 3, which is based directly on the strain energy function, must be modified. A clue to how constraints in such materials can be dealt with is suggested by Remark (b) in Section 3, where it was observed that the component $\mathbf{S}_{\|}$ of stress in a constrained Green-elastic material is uniquely defined (by (20)) at each point of the constraint manifold. Thus, we will suppose that for a Cauchy-elastic material subject to the internal constraint (2), the surface component of the stress $\mathbf{S}$ is given by a constitutive function $\mathbf{S}'$:

$$\mathbf{S}_{\|} = \mathbf{S}'(\mathbf{E}), \quad \mathbf{E} \in \mathcal{S}. \tag{21}$$

Again, we take $\mathbf{S}$ to be independent of strain-rate. Further, we assume that for any Cauchy-elastic material whose surface component of stress matches $\mathbf{S}'$ on $\mathcal{S}$, the stress power of the Cauchy-elastic material during any motion that satisfies the constraint is equal to the stress power of the constrained Cauchy-elastic material. For any matching Cauchy-elastic material, we then have

$$\bar{\mathbf{S}} \cdot \dot{\mathbf{E}} = \mathbf{S} \cdot \dot{\mathbf{E}} = \mathbf{S}' \cdot \dot{\mathbf{E}} \tag{22}$$

for all $\dot{\mathbf{E}}$ satisfying (3). Consequently, the stress in the constrained material is of the form

$$\begin{aligned} \mathbf{S} &= \bar{\mathbf{S}} + \lambda \frac{\partial \phi}{\partial \mathbf{E}} \\ &= \mathbf{S}' + \bar{\lambda} \frac{\partial \phi}{\partial \mathbf{E}}, \quad \mathbf{E} \in \mathcal{S} \end{aligned} \tag{23}$$

where $\bar{\lambda}$ and λ are Lagrange multipliers.

Again, we can start out with any Cauchy-elastic constitutive function $\bar{\mathbf{S}}$, specialize it to $\mathcal{S}$, add on an arbitrary part orthogonal to $\mathcal{S}$, and thereby obtain the corresponding internally constrained material.

References

Adkins, J. E., 1961, "Large Elastic Deformations," *Progress in Solid Mechanics*, Vol. II, I. N. Sneddon and R. Hill, eds., North-Holland, Amsterdam, pp. 1–60.

Antman, S. S., and Marlow, R. S., 1991, "Material Constraints, Lagrange Multipliers, and Compatibility. Applications to Rod and Shell Theories," *Archive for Rational Mechanics and Analysis*, Vol. 116, pp. 257–299.

Beatty, M. F., 1987, "Topics in Finite Elasticity: Hyperelasticity of Rubber, Elastomers, and Biological Tissues—With Examples," ASME *Applied Mechanics Reviews*, Vol. 40, pp. 1699–1734.

Beatty, M. F., and Hayes, M. A., 1992, "Deformations of an Elastic, Internally Constrained Material. Part I: Homogeneous Deformations," *Journal of Elasticity*, Vol. 29, pp. 1–84.

Carlson, D. E., and Tortorelli, D. A., 1994, "On Hyperelasticity with Internal Constraints," *Recent Advances in Engineering Science: Proceedings of the 31st Annual Technical Meeting of the Society of Engineering Science*, Oct. 10–12, Texas A & M University, D. H. Allen and D. C. Lagoudas, eds.; abstract is missing; completed paper to appear in *Journal of Elasticity*.

Carlson, D. E., and Tortorelli, D. A., 1994b, "On the Theory of Thermoelasticity in the Presence of Internal Constraints," *Abstracts of Contributed Papers: Twelfth U.S. National Congress of Applied Mechanics*, June 27–July 1, University of Washington, Seattle, p. 125.

Casey, J., 1994, "Geometrical Derivation of Lagrange's Equations for a System of Particles," *American Journal of Physics*, Vol. 62, p. 836–847.

Cohen, H., and Wang, C.-C., 1987, "On the Response and Symmetry of Elastic Materials with Internal Constraints," *Archive for Rational Mechanics and Analysis*, Vol. 99, pp. 1–36.

Ericksen, J. L., and Rivlin, R. S., 1954, "Large Elastic Deformations of Homogeneous Anisotropic Materials," *Journal of Rational Mechanics and Analysis*, Vol. 3, pp. 281–301.

Green, A. E., and Adkins, J. E., 1960, *Large Elastic Deformations and Non-Linear Continuum Mechanics*, Clarendon Press, Oxford, U.K.

Green, A. E., and Naghdi, P. M., 1977, "A Note on Thermodynamics of Constrained Materials," ASME JOURNAL OF APPLIED MECHANICS, Vol. 44, p. 787.

Green, A. E., Naghdi, P. M., and Trapp, J. A., 1970, "Thermodynamics of a Continuum with Internal Constraints," *International Journal of Engineering Science*, Vol. 8, pp. 891–908.

Gurtin, M. E., and Podio-Guidugli, P., 1973, "The Thermodynamics of Constrained Materials," *Archive for Rational Mechanics and Analysis*, Vol. 51, pp. 192–208.

Podio-Guidugli, P., and Vianello, M., 1989, "Constraint Manifolds for Isotropic Solids," *Archive for Rational Mechanics and Analysis*, Vol. 105, pp. 105–121.

Rivlin, R. S., 1956, "Large Elastic Deformations," *Rheology: Theory and Applications*, Vol. 1, F. R. Eirich, ed., Academic Press, New York, pp. 351–385.

Rivlin, R. S., 1960, "Some Topics in Finite Elasticity," *Structural Mechanics: Proceedings of the 1st Symposium on Naval Structural Mechanics*, Aug. 11–14, Stanford University, J. N. Goodier, and N. J. Hoff, eds., Pergamon Press, New York, pp. 169–198.

Truesdell, C., and Noll, W., 1965, "The Non-Linear Field Theories of Mechanics," *Handbuch der Physik*, S. Flügge, ed., Vol. III/3, Springer-Verlag, New York, pp. 1–602.

Wang, C.-C., 1979, *Mathematical Principles of Mechanics and Electromagnetism—Part A: Analytical and Continuum Mechanics*, Plenum Press, New York.

[10] It is worth pointing out also that when (8) is evaluated on $\mathcal{S}$, the two terms on the right-hand side become orthogonal to one another: the first one lies in the tangent space to $\mathcal{S}$ and the second one is orthogonal to $\mathcal{S}$.

Divergence Instability of a Spinning Disk With Axial Spindle Displacement in Contact With Evenly Spaced Stationary Springs

Jen-San Chen[1,3] and Cheng-Chou Wong[2,3]

The titled problem is studied numerically by finite element calculation and analytically by three-mode eigenfunction expansion. It is found that divergence instability of the coupled system is

[1] Associate Professor.

[2] Graduate Student.

[3] Department of Mechanical Engineering, National Taiwan University, Taipei, Taiwan 107, R.O.C.

Contributed by the Applied Mechanics Division of THE AMERICAN SOCIETY OF MECHANICAL ENGINEERS for publication in the ASME JOURNAL OF APPLIED MECHANICS. Manuscript received by the ASME Applied Mechanics Division, Sept. 26, 1994; final revision, Nov. 14, 1994. Associate Technical Editor: F. Y. M. Wan.

induced only when two times the number of nodal diameters 2n *is equal to a multiple of the number of stationary springs* N, *but* n *itself is not a multiple of* N.

Introduction

It has been known in the wood cutting industry that allowing the central clamping collar of the circular saw to slide freely along the axis of rotation can improve the stability of the cutting process. Mote's paper (1977), in which the collar was modeled as a line mass without stiffness, appears to be the first publication trying to explain the effects of the rigid-body translation on the stability of the floating circular saw. Mote's model failed to explain the observed improvement in stability that occurs by allowing the collar to slide freely, so Price (1987) extended Mote's model by considering the disk and collar system as an elastic plate with two concentric regions of different thickness. As the thickness ratio of the collar and plate becomes very large, Price's calculations show that the divergence instability induced by load system stiffness can be eliminated. These papers are mainly concerned with the dynamics of a spinning disk with axial spindle displacement in contact with a *single* stationary load system. In the wood cutting industry, however, the saw blade is usually restrained from lateral vibration by the presence of more than one guide pad. This Note presents the calculation results and analytical verification on the divergence instability of a spinning disk with axial spindle displacement in contact with multiple stationary springs.

Equations of Motion

The motion of a spinning flexible disk with axial translation can be described in two coordinates frames. The local frame *o-xyz* is attached to the rigid, massless collar and translates in the Z-direction relative to the inertial frame *O-XYZ*. Both the Z- and the z-axes are coincident with the rotation axis of the floating circular disk. The disk is clamped by the collar on the inner radius $r = a$ and free on the outer radius $r = b$. The position of the collar is measured by Z from the origin O. The elastic transverse displacement w of the disk is measured with respect to the local *o-xyz* frame. The disk rotates about the *oz*-axis with constant rotation speed Ω and is in contact with N evenly spaced point springs. By D'Alembert's principle, the equation of motion of the disk in terms of w and with respect to the nonrotating local coordinate system (r, θ) can be written as

$$\rho h\left(w_{,tt} + 2\Omega w_{,t\theta} + \Omega^2 w_{,\theta\theta}\right) + D\nabla^4 w - \frac{h}{r}(\sigma_r r w_{,r})_{,r} - \frac{h\sigma_\theta}{r^2} w_{,\theta\theta} + \rho h\ddot{Z} = -\sum_{j=1}^{N} \frac{k_z}{r}\delta(r-\xi)\delta(\theta-\theta_j)(w+Z). \quad (1)$$

The parameters ρ, h, and D are the mass density, thickness, and flexural rigidity of the disk, respectively. $\delta(\cdot)$ is the Dirac delta function. The point springs are evenly located on a circle with radius $r = \xi$, where $a \le \xi \le b$. The membrane stresses σ_r and σ_θ are due to the centrifugal effect.

By considering the force balance in the Z-direction between the total inertial force on the disk and the forces exerted by the stationary springs k_z, one can obtain an additional equation of motion

$$m\ddot{Z} + \int_0^{2\pi}\int_a^b \rho h w_{,tt} r dr d\theta + \sum_{j=1}^{N} k_z\left[w(\xi,\theta_j) + Z\right] = 0 \quad (2)$$

where m is the mass of the circular plate.

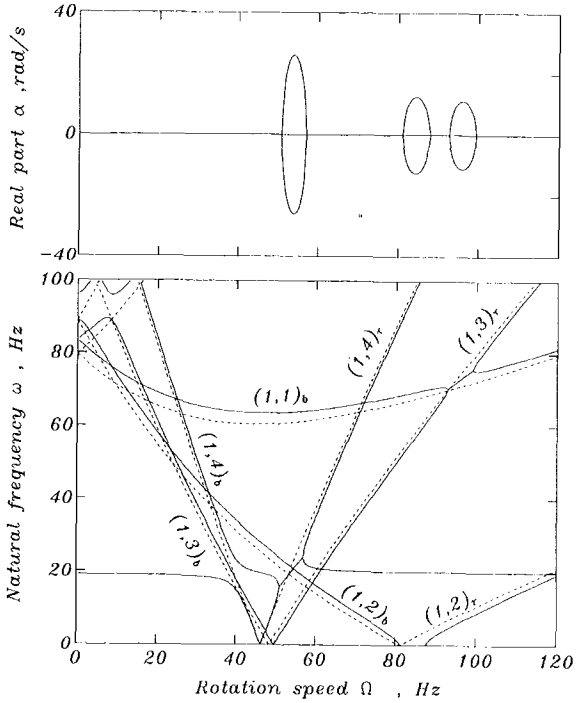

Fig. 1 Eigenvalues of the spinning disk in contact with four stationary springs k_z = 3000 N / m

Numerical Results

The eigenvalues of the coupled system are obtained by a finite element computation which is similar to the one presented in Ono et al. (1991). The material properties of the disk used in the calculations are $\rho = 7.84 \times 10^3 \text{kg/m}^3$, $D = 19.36$ Nm, $h = 1.02$ mm, $a = 101.6$ mm, $b = 203.2$ mm. Figure 1 shows the cases when the spinning disk is in contact with four evenly spaced stationary springs k_z at the radial position $\xi = 0.9b$. The ordinates are the natural frequency ω and the real part α of the eigenvalue ($\lambda = \alpha + i\omega$). The solid lines represent the cases for stiffness $k_z = 3000$ N/m. The dashed lines correspond to the case of a freely spinning disk with rigid-body translation (i.e., $k_z = 0$). Attention is focused on the divergence instability when a backward wave meets its complex conjugate near the critical speed. Figure 1 shows that divergence instability is induced when $(1, 2)_b$ meets its complex conjugate, but no divergence instability is induced when $(1, 3)_b$ and $(1, 4)_b$ meet their complex conjugates. Mode label $(m, n)_b$ represents a backward wave with m nodal circles and n nodal diameters. Subscripts "f" and "r" in the mode label in Fig. 1 represent a forward and a reflected wave, respectively. From these observations and additional calculations not shown here it is found that divergence instability is induced when $2n$ is equal to a multiple of N and n itself is not a multiple of N.

In order to study the behavior of divergence instability as k_z changes, we consider the case when Ω is fixed at 85 Hz, just higher than the critical speed $\Omega_c = 81$ Hz of mode (1, 2). The solid lines in Figs. 2(*a*), (*b*), and (*c*) show the eigenvalue λ as a function of k_z when $N = 2$, 3, and 4, respectively. In Fig. 2(*a*), the two eigenvalues are purely imaginary except when $k_z^- < k_z < k_z^+$. When $k_z^- < k_z < k_{z_f}^+$, the eigenvalues are complex numbers. In Fig. 2(*b*) the two eigenvalues are always purely imaginary, with one increasing monotonically with k_z and the other decreasing as k_z increases until $k_z = k_z^*$. As $k_z > k_z^*$ this eigenvalue increases from zero as k_z increases. This represents the phenomenon that critical speed increases in the $\lambda - \Omega$ diagram when k_z increases. In Fig. 2(*c*) one of

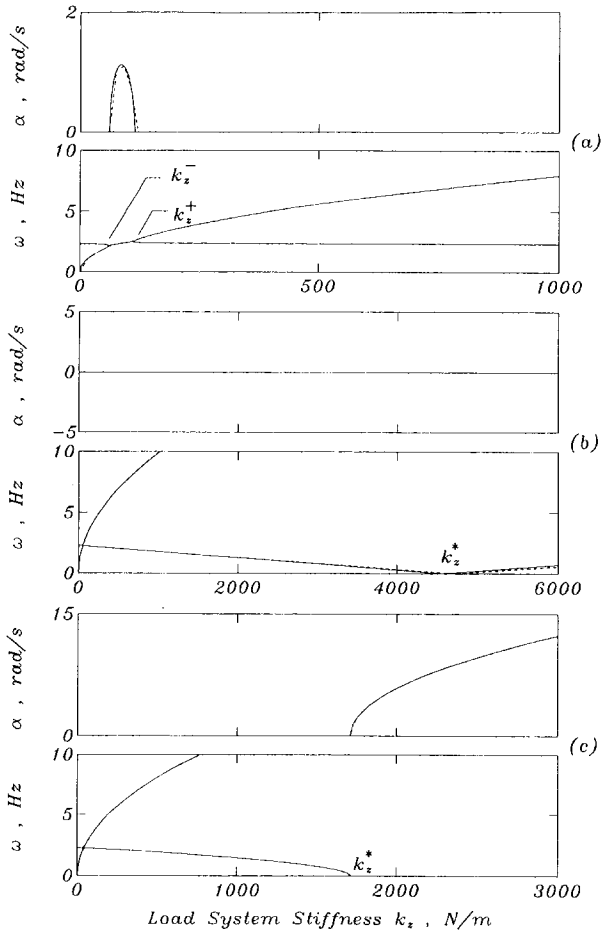

Fig. 2 Relation between eigenvalues and stiffness k_z when the disk is spinning at Ω = 85 Hz and in contact with (a) two, (b) three, and (c) four springs, respectively

the eigenvalues is always purely imaginary and the other becomes a real number when $k_z > k_z^*$. This means that the divergence instability is induced when $k_z > k_z^*$.

Eigenfunction Expansion Method

Equations (1) and (2) can be rewritten in the matrix operator form

$$\mathbf{M}\mathbf{u}_{,tt} + \mathbf{G}\mathbf{u}_{,t} + (\mathbf{K} + \hat{\mathbf{K}})\mathbf{u} = \mathbf{0}, \tag{3}$$

where the vector $\mathbf{u}$ is defined as $\mathbf{u} \equiv \begin{Bmatrix} w \\ Z \end{Bmatrix}$. The matrix operators **M**, **G**, and **K** are associated with the freely spinning disk, while $\hat{\mathbf{K}}$ is associated with the stationary point springs. The inner product between two eigenvectors $\mathbf{u}_1$ and $\mathbf{u}_2$ is defined as

$$\langle \mathbf{u}_1, \mathbf{u}_2 \rangle = \int_0^{2\pi} \int_a^b \bar{w}_1 w_2 r dr d\theta + \bar{Z}_1 Z_2. \tag{4}$$

the overbar means complex conjugate. The orthogonality relations among eigenfunctions of a freely spinning disk with respect to operators **M**, **G**, and **K** in Eq. (3) have been established in Wong (1994).

In order to study the eigenvalue changes near the critical speed, we express the eigenfunction of Eq. (3) in terms of the eigenfunctions of three neighboring modes of the freely spinning disk

$$\mathbf{u} = c_1 \mathbf{u}_{mn} + c_2 \bar{\mathbf{u}}_{mn} + c_3 \mathbf{u}_{00} \tag{5}$$

where $\mathbf{u}_{mn} = \begin{Bmatrix} w_{mn} \\ 0 \end{Bmatrix}$ and $\mathbf{u}_{00} = \begin{Bmatrix} 0 \\ 1 \end{Bmatrix}$. $w_{mn} = R_{mn}(r)e^{in\theta}$ is the eigenfunction of the mode (m, n) with $n \neq 0$, whose natural frequency is ω_{mn}. $R_{mn}(r)$ is a real-valued function of r. Substituting Eq. (5) into (3) and taking the inner product between each of the three eigenfunctions and both sides of Eq. (3) with use of the orthogonality properties described in Wong (1994), we obtain a system of three homogeneous linear algebraic equations with unknowns c_1, c_2, and c_3. For the existence of nontrivial solutions the determinant of the coefficient matrix should vanish. Consequently, the eigenvalue λ can be obtained by solving the following equation:

$$\alpha_0\lambda^6 + (\beta_0 + \beta_1\epsilon)\lambda^4 + (\gamma_0 + \gamma_1\epsilon + \gamma_2\epsilon^2)\lambda^2 + (\eta_1\epsilon + \eta_2\epsilon^2 + \eta_3\epsilon^3) = 0 \tag{6}$$

where

$$\alpha_0 = 4AR_{mn}^{*2}, \quad \beta_0 = 4A(S_{mn}^2 + R_{mn}^{*2}\omega_{mn}^2),$$

$$\beta_1 = 4R_{mn}^* N[R_{mn}^* + AR_{mn}^2(\xi)],$$

$$\gamma_0 = 4A\omega_{mn}^2 S_{mn}^2,$$

$$\gamma_1 = 4N[S_{mn}^2 + R_{mn}^{*2}\omega_{mn}^2 + R_{mn}^2(\xi)A\omega_{mn}S_{mn}],$$

$$\gamma_2 = R_{mn}^2(\xi)[4R_{mn}^*(N^2 - \kappa_1) + R_{mn}^2(\xi)A(N^2 - \kappa_2)],$$

$$\eta_1 = 4N\omega_{mn}^2 S_{mn}^2,$$

$$\eta_2 = 4R_{mn}^2(\xi)\omega_{mn}S_{mn}(N^2 - \kappa_1),$$

$$\eta_3 = R_{mn}^4(\xi)[N^3 - (2\kappa_1 + \kappa_2)N + \kappa_3]$$

and

$$\epsilon = k_z/\rho h, \quad A = \pi(b^2 - a^2), \quad R_{mn}^* = \pi\int_a^b R_{mn}^2(r)rdr,$$

$$S_{mn} = \pi R_{mn}^*(2n\Omega + \omega_{mn}), \quad \kappa_1 = \sum_{j=1}^{N}\sum_{k=1}^{N} e^{2in\pi(j-k)/N},$$

$$\kappa_2 = \sum_{j=1}^{N}\sum_{k=1}^{N} e^{4in\pi(j-k)/N},$$

$$\kappa_3 = \sum_{j=1}^{N}\sum_{k=1}^{N}\sum_{l=1}^{N} 2\cos\left[\frac{2n\pi(2l - j - k)}{N}\right].$$

The roots of Eq. (6) are solved and plotted as dashed lines in Fig. 2. It can be seen that the three-mode expansion is an excellent approximation to the finite element solution.

Case I. Neither n nor $2n$ is a multiple of N. In this case $\kappa_1 = \kappa_2 = \kappa_3 = 0$. The eigenvalues can be solved as

$$\lambda_0^2 = -\frac{\epsilon N}{A} \quad \text{and} \quad \lambda_\pm^2 = -(G + H) \pm 2\sqrt{GH}$$

where G and H are two positive real numbers

$$G = n^2\Omega^2, \quad H = (n\Omega + \omega_{mn})^2 + \frac{\epsilon NR_{mn}^2(\xi)}{2R_{mn}^*}.$$

It is clear that all the eigenvalues remain purely imaginary as the stiffness parameter ϵ changes. λ_0 corresponds to the mode with frequency proportional to $\sqrt{k_z}$ in Fig. 2(*b*). λ_+ corresponds to the mode with frequency decreasing to zero as k_z increases. λ_+ changes sign when $\epsilon = \epsilon^* = -\frac{2S_{mn}\omega_{mn}}{NR_{mn}^2(\xi)}$, which corresponds to k_z^* in Fig. 2(*b*). λ_- is an extra root and corresponds to mode $(m, n)_f$, whose natural frequency is beyond the range of Fig. 2. Therefore no diver-

gence instability will be induced by the stationary springs in this case.

Case II. $2n$ is a multiple of N, but n itself is not a multiple of N. In this case $\kappa_1 = \kappa_3 = 0$, and $\kappa_2 = N^2$. The eigenvalues can be solved as

$$\lambda_0^2 = -\frac{\epsilon N}{A} \quad \text{and}$$

$$\lambda_\pm^2 = -(G+H) \pm 2\sqrt{GH + \frac{\epsilon^2 N R_{mm}^2(\xi)}{16 R_{mn}^{*2}}}.$$

It is obvious that λ_0^2 and λ_-^2 are always negative and correspond to stable modes. On the other hand the sign of λ_+^2 depends on ϵ. It can be shown that λ_+^2 becomes positive when $\epsilon > \epsilon^* = -\frac{S_{mn}\omega_{mn}}{N R_{mn}^2(\xi)}$. The eigenfunction corresponding to positive λ_+^2 is an unstable mode with zero natural frequency. In other words, divergence instability is induced in this case. It is noted that ϵ^* corresponds to k_z^* in Fig. 2(*c*).

Case III. n is a multiple of N. In this case $\kappa_1 = \kappa_2 = N^2$ and $\kappa_3 = 2N^3$. It is difficult to derive the explicit expression for λ^2 in this case. However, we can show that the roots for λ^2 are one negative real number and two complex conjugate numbers when $\epsilon_-^* < \epsilon < \epsilon_+^*$, where

$$\epsilon_\pm^* = \frac{A\omega_{mn}^2\left[2P - Q \pm \sqrt{Q(-8P+Q)}\right]}{2N(P+Q)}$$

$$P = R_{mn}^*(n\Omega + 4\omega_{mn}), \quad Q = A\omega_{mn}R_{mn}^2(\xi)$$

The real λ^2 corresponds to the stable mode $(m, n)_f$. The eigenfunctions corresponding to complex conjugate λ^2 are two modes with the same nonzero natural frequency, one with positive and the other with negative real parts. Therefore merged-type instability occurs in this case. It is noted that $\epsilon_\pm^*$ correspond to $k_z^\pm$ in Fig. 2(*a*).

References

Mote, C. D., Jr., 1977, "Moving Load Stability of a Circular Plate on a Floating Central Collar," *Journal of the Acoustical Society of America*, Vol. 61, pp. 439–447.

Ono, K., Chen, J.-S., and Bogy, D. B., 1991, "Stability Analysis for the Head-Disk Interface in a Flexible Disk Drive," ASME JOURNAL OF APPLIED MECHANICS, Vol. 58, pp. 1005–1014.

Price, K. B., 1987, "Analysis of the Dynamics of Guided Rotating Free Center Plates," Ph.D. dissertation, University of California, Berkeley, CA.

Wong, C.-C., 1994, "Vibration and Stability of a Spinning Disk in Contact With Evenly Spaced Stationary Load Systems," Master Thesis, Department of Mechanical Engineering, National Taiwan University, Taipei, Taiwan.

Radial Stresses in Composite Thick-Walled Shafts

Naki Tutuncu[1]

Introduction

Increasing use of thick-walled composite tubes as machine elements necessitates the investigation of through-the-thickness stresses. These stresses might be due to externally applied loads such as pressure, torque or axial force, or due to thermal loads. A possible case which includes all of the above is presented by Tutuncu and Winckler (1993) with the assumptions that the cylindrical tube is long, i.e., no end effects are considered, and stresses and strains are independent of the circumferential coordinate. Based on the same assumptions, the present paper will address the problem of determining radial stresses in composite rotating shafts resulting solely from centrifugal forces which constitute the body force in radial direction.

In conventional applications of cylindrical tubes as hollow shafts, the radial stresses may rightfully be neglected for they are of much less magnitude as compared with axial and hoop stresses. In laminated structures, however, these stresses may be of great concern because the transverse strength of a typical laminate is much less than its axial strength. Assuming the strength in radial direction is approximately equal to the transverse strength, a relatively small radial stress might cause delamination in the structure.

A displacement based linear elasticity approach will be presented. The tubes in question may be multilayered allowing the possibility of each layer being made of a different orthotropic material placed at an arbitrary angle to the tube axis. For a complete discussion of stresses in thick-walled tubes with the absence of body forces the reader is referred to the papers by Pagano and Halpin (1968), Hyer, Cooper, and Cohen (1986), Hyer and Rousseau (1987), and Tutuncu and Winckler (1993).

Differential Equation and Boundary Conditions. Consider a helical wound composite cylinder which is rotating at an angular velocity ω. As a result of the assumptions made, the problem is reduced to a planar elasticity problem where the radial, circumferential, and axial displacements are given, respectively, as follows:

$$u_r = u(r), \quad u_\theta = v(z,r), \quad u_z = w(z,r). \tag{1}$$

The strain-displacement relations reduce to

$$\epsilon_r = \frac{du}{dr}, \quad \epsilon_\theta = \frac{u}{r}, \quad \epsilon_z = \frac{\partial w}{\partial z}, \quad \gamma_{r\theta} = \frac{\partial v}{\partial r} - \frac{v}{r},$$

$$\gamma_{\theta z} = \frac{\partial v}{\partial z}, \quad \gamma_{zr} = \frac{\partial w}{\partial r}. \tag{2}$$

The equilibrium equation in radial direction is

$$\frac{d\sigma_r}{dr} + \frac{\sigma_r - \sigma_\theta}{r} + \omega^2 \rho r = 0 \tag{3}$$

where $\omega^2\rho r$ is the body force per unit volume and ρ is the density of the material.

On the account of the fact that all stresses are considered to be functions of r only and the boundary conditions $\tau_{rz} = \tau_{r\theta} = 0$ at $r = R_i$, the shearing stresses τ_{rz} and $\tau_{r\theta}$ vanish, and the remaining two equilibrium equations, with the absence of body forces in axial and circumferential directions, are identically satisfied. The constitutive relation is then written as

$$\begin{Bmatrix} \sigma_r \\ \sigma_\theta \\ \sigma_z \\ \tau_{\theta z} \end{Bmatrix} = \begin{bmatrix} C_{11} & C_{12} & C_{13} & C_{14} \\ C_{12} & C_{22} & C_{23} & C_{24} \\ C_{13} & C_{23} & C_{33} & C_{34} \\ C_{14} & C_{24} & C_{34} & C_{44} \end{bmatrix} \begin{Bmatrix} \epsilon_r \\ \epsilon_\theta \\ \epsilon_z \\ \gamma_{\theta z} \end{Bmatrix}. \tag{4}$$

Note that in cross-ply laminates, the extension-shear coupling terms C_{14}, C_{24}, C_{34} would not appear. Following the steps outlined by Tutuncu and Winckler (1993), the circumferential and axial displacements are found as follows:

[1]Assistant Professor, Department of Mechanical Engineering, Çukurova University, 01330 Adana, Turkey.

Contributed by the Applied Mechanics Division of THE AMERICAN SOCIETY OF MECHANICAL ENGINEERS for publication in the ASME JOURNAL OF APPLIED MECHANICS. Manuscript received by the ASME Applied Mechanics Division, July 7, 1994; final revision, Dec. 29, 1994. Associate Technical Editor: G. J. Dvorak.